Journal of Microscopy, Vol. 203, Pt 3, September 2001, pp. 303–313.
Received 28 March 2000; accepted 6 December 2000

On the analysis of spatial binary images

C. LANG*, J. OHSER† & R. HILFER‡
**Freiberg University of Mining and Technology, Institute of Computer Science, D-09596 Freiberg, Germany*
†Institute of Industrial Mathematics, Erwin-Schrödinger-Strasse, D-67663 Kaiserslautern, Germany
‡Institute for Computer Applications, University of Stuttgart, Pfaffenwaldring 27, D-70569 Stuttgart, Germany and Institute of Physics, University of Mainz, D-55099 Mainz, Germany

Key words. Connectivity, Euler number, integral geometry, integral of Gaussian curvature, integral of mean curvature, quermassdensities, spatial image analysis, stochastic geometry, surface density, tomography.

Summary

This paper deals with the analysis of spatial images taken from microscopically heterogeneous but macroscopically homogeneous microstructures. A new method is presented, which is strictly based on integral-geometric formulae such as Crofton's intersection formulae and Hadwiger's recursive definition of the Euler number. By means of this approach the quermassdensities can be expressed as the inner products of two vectors where the first vector carries the 'integrated local knowledge' about the microstructure and the second vector depends on the lateral resolution of the image as well as the quadrature rules used in the discretization of the integral-geometric formulae. As an example of application we consider the analysis of spatial microtomographic images obtained from natural sandstones.

1. Introduction

Components (or phases) of microstructures are usually considered as sets which may have 'smooth surfaces' almost everywhere. (In the simplest case a component is described by a locally finite union of compact convex sets, see, e.g. Schneider, 1993.) We assume that the structure is microscopically heterogeneous but macroscopically homogeneous, i.e. a component α is modelled as a macroscopically homogeneous random set. The homogeneity of α allows us to introduce the following geometric characteristics: the volume density, the surface density, the specific integral of mean curvature, and the specific integral of total curvature.

Correspondence: J. Ohser. Tel: + 49(0)631 3668125;
e-mail: ohser@itwm.uni-kl.de

These quantities play a central role in the quantitative characterization of microstructure components. Up to multiplicative constants, these geometric characteristics are the densities of the (random) quermassintegrals defined for a homogeneous random set, and the list of the four geometric characteristics is complete in some sense (cf. Hadwiger's characterization theorem, see, e.g. Schneider, 1993; pp. 210f). Procedures for estimating the quermassdensities are based on Crofton's intersection formulae, see Schneider (1993), p. 235, as well as a modification of Hadwiger's recursive definition of the Euler number, see Ohser & Nagel (1996) and Nagel *et al.* (2000).

In recent years, a generalized geometric characterization based on the volume density, the surface density, and the densities of the two curvature integrals was suggested for the geometric treatment of porous and heterogeneous media in physics (see Hilfer, 1992a, b; 1996). These geometric characteristics can be readily incorporated into the mean field approximation for the microscopic boundary value problems describing transport phenomena in these media. It seems that the resulting parameter-free predictions are in good agreement with experiment, see Widjajakususina *et al.* (1999).

The component α is observed in a cuboidal lattice of points, i.e. we consider spatial digital images of the microstructure. The discrete version of a (random) set forms a (random) binary digital image. Depending on whether a lattice point is in α or in its complementary set, this point is assigned the Boolean values 1 or 0, respectively. The selection can be performed, e.g. by thresholding brightness values to separate the α-phase from the background.

For the purpose of application in image analysis, the integrals that occur in the Crofton's intersection formulae and Hadwiger's recursive definition are discretized in such a

way that 'measurement' of the geometric characteristics can be performed by simple 'counting' of elements in a digital image where the elements are voxels or neighbourhood configurations of voxels. The observation of the structure in a point lattice implies a corresponding discretization of the integral-geometric formulae.

A very powerful technique of image processing is filtering of digital images, but filtering can also be applied as a tool of image analysis. The statistical estimation of the quermass-densities suggested in the following includes linear filtering of the binary image as a basic tool. The algorithm presented in this paper consists of three steps:

1 Filtering of the binary image (the 'labelling of neighbourhood configurations' in the binary image),

2 generating the vector of absolute frequencies of neighbourhood configurations (the 'integration step'), and

3 estimating the geometric characteristics from the absolute frequencies of configurations (the 'analysis step').

By means of filtering, each neighbourhood configuration in a binary image is assigned an integer. Thus, the result of the filtering is an image of integer valued voxels. The generation of the absolute frequencies of configurations can be understood as a discretized version of the computation of the translative integrals occurring in Crofton's intersection formulae, and the vector of absolute frequencies carries the 'complete information' of the image about the quermass-densities; it can be used as the data base of statistical estimation. As the neighbourhood configurations are represented by 'grey-tones', the vector of absolute frequencies of the neighbourhood configuration in the binary image is nothing other than the vector of the absolute frequencies of grey-tones in the filtered image.

2. The continuous case: integral-geometric formulae

Firstly, we review some integral-geometric formulae widely used in image analysis. We consider a set X of the 3-dimensional space that belongs to the convex ring, i.e. X is a finite union of compact convex sets. Set X can be understood as a particle of a microstructure: functionals of X are commonly referred to as particle parameters. We are interested in the quermassintegrals of X, which are up to multiplicative constants the volume $V(X)$, the surface area $S(X)$, the integral of the mean curvature $M(X)$, and the Euler number $\chi^3(X)$. We remark that $K(X) = 4\pi\chi^3(X)$ is the integral of the total curvature of X. (The upper index indicates the dimension of space on which the functionals are defined.)

Let E_x denote a plane in space depending on the parameter $x \in \mathbb{R}^3$. We introduce spherical polar coordinates $x = (r, \omega)$ where ω represents the normal direction of the plane and r is the distance of the plane from the origin. It is convenient to identify the direction $\omega = (\vartheta, \varphi)$ to be a point on the positive half sphere where $r \in \mathbb{R}$ represents the intersection point of the plane E with a straight line orthogonal to E and passing through the origin; define $E_{r,\omega} := E_{-r,-\omega}$ for $r < 0$. The intersection $X \cap E_{r,\omega}$, of a spatial object X and the plane $E_{r,\omega}$ is said to be a 2-dimensional section or a planar section of the object X.

A straight line e in the 3-dimensional space can be characterized by the Euler angles $(\phi, \vartheta, \varphi)$ and its distance r from the origin or, alternatively, by the direction $\omega = (\vartheta, \varphi)$ describing the direction of the straight line in space and the point $y = (r, \phi) \in \mathbb{R}^2$ that represents the intersection point of e with a plane $E_{O,\omega}$ orthogonal to e. Thus, we write $e = e_{r,\phi,\vartheta,\varphi}$ or, equivalently $e = e_{y,\omega}$ for a parametric representation of a straight line in 3-dimensional space; $e_{r,\phi,\vartheta,\varphi} := e_{-r,-\phi,\vartheta,\varphi}$ for $r < 0$. The intersection $X \cap e_{y,\omega}$ is said to be a 1-dimensional section or a linear section of X. Because X is not necessarily a convex set a linear section of X can consist of a family of chords.

A '0-dimensional section' is obtained when intersecting the set X with a set $\{x\}$ that consists only of the point $x \in \mathbb{R}^3$. If the point x is covered by the set X then $X \cap \{x\} = \{x\}$ and, otherwise, this intersection is empty, $X \cap \{x\} = \emptyset$.

By means of Crofton's formulae, the functionals of a 3-dimensional set X are expressed in terms of the functionals defined for lower-dimensional sections. For a 2-dimensional section, let A, L^2, and χ^2 denote the area, the boundary length, and the planar Euler-number, respectively. Notice that $C = 2\pi\chi^2$ is the integral of curvature. A linear section of the set X can consist of a family of chords; L and χ^1 are their total length and the chord number, respectively. Finally, we introduce the Euler number χ^0 of a 0-dimensional section. A survey of the Crofton formulae is given in Table 1.

Consider now a pair of parallel section planes $E_{r,\omega}$ and $E_{r+\Delta,\omega}$ having the distance Δ. We give formulae that link the Euler number of a spatial set to functionals of section profiles observed in pairs of parallel sections. Denote $Y_r = (X \cap E_{r,\omega})_{-(r,\omega)}$ the section profiles shifted (or projected) onto the plane $E_{0,\omega}$, where $X_{-(\Delta,\omega)}$ means the translation of X by $-(\Delta,\omega) \in \mathbb{R}^3$. The sets Y_r and $Y_{r+\Delta}$ are assigned to the section profiles of X obtained by the intersection with the planes $E_{r,\omega}$ and $E_{r+\Delta,\omega}$; both sets are subsets of the same plane $E_{0,\omega}$ and operations like union or intersection of them are well-defined. Consider a d-dimensional set X belonging to the convex ring. If the set X is morphologically open and closed with respect to the segment $s_{\Delta,\omega} = [o,(\Delta,\omega)]$, Hadwiger's recursive definition of the Euler number can be rewritten as

$$\chi^d(X) = \frac{1}{\Delta}\int[\chi^{d-1}(Y_r \cup Y_{r+\Delta}) - \chi^{d-1}(Y_r)]\,dr \qquad (1)$$

and, equivalently,

$$\chi^d(X) = \frac{1}{\Delta}\int[\chi^{d-1}(Y_r) - \chi^{d-1}(Y_r \cap Y_{r+\Delta})]\,dr \qquad (2)$$

Table 1. Survey of the functionals defined for three-dimensional sets. The measure μ is the rotation invariant measure on the unit sphere Ω with $\mu(\Omega) = 4\pi$. By means of Crofton's formulae, these functionals are represented by their counterparts defined on lower dimensional spaces. Notice that $K(X) = 4\pi\chi(X)$. The innermost integrals are over the orthogonal spaces of $E_{0,\omega}$ and $e_{0,\omega}$, respectively, and the outer integrals are over the unit sphere Ω in ω. The innermost integral $\wp^{\omega}(X) := \int \chi(X \cap e_{y,\omega})\, dy$ is the specific total projection of α.

$d = 3$	$d = 2$	$d = 1$	$d = 0$
V(X)	$= \int A(X \cap E_{r,\omega})\, dr$	$= \int L(X \cap e_{y,\omega})\, dy$	$= \int \chi(X \cap \{x\})\, dx$
S(X)	$= \frac{4}{\pi} \int\int L(X \cap E_{r,\omega})\, dr\mu(d\omega)$	$= 4 \int\int \chi(X \cap e_{y,\omega})\, dy\mu(d\omega)$	
M(X)	$= 2\pi \int\int \chi(X \cap E_{r,\omega})\, dr\mu(d\omega)$		
K(X)			

with the initial setting $\chi^0(\{0\}) = 0$ and $\chi^0(\emptyset) = 1$, see Ohser & Nagel (1996) and Nagel *et al.* (2000). The integrals are over the orthogonal space of the $d - 1$-dimensional hyperplane $E_{r,\omega}$. By means of these recursive formulae, the Euler number χ^d defined on d-dimensional space can be expressed in terms of the Euler number defined on lower-dimensional spaces.

3. Neighbourhood configurations in binary images

Turn now to homogeneous structures. Instead of a bounded deterministic set X we will consider a sample of an unbounded random set α observed in a bounded spatial window W. It is assumed that α is homogeneous (i.e. its distribution is invariant with respect to translations). Furthermore, we assume that realizations of α are − with probability one − locally finite unions of compact convex sets.

To guarantee the unbiasedness of estimators introduced in the following, we will often suppose that α is almost surely morphologically open as well as morphologically closed with respect to all segments of the set S containing all (closed) edges, faces' diagonals, and space diagonals of the unit cell of the lattice used in the discretication of α. The zonotope obtained as the Minkowski sum of all segments $s \in S$ is the smallest set having this property. We remark that some surface rendering algorithms applied in computer graphics generate polygonal surfaces (e.g. triangulation by the wrapper algorithm, see Lohmann, 1998) such that the corresponding sets are morphologically open and morphologically closed with respect to all segments in S. As a consequence, the random set α has a polygonal surface where the edges of the polygons are of the form $rs + x$ for $r \geq 1$, $s \in S$ and $x \in \mathbb{R}^3$. Hence, α as well as the closure of the complementary set α^c are locally finite unions of compact convex sets having nonempty interior.

It is convenient to estimate the densities of the quermass-integrals introduced in the previous section. Our choice for the notation is the same as suggested by the early school of stereology: V_V denotes the volume density of α, S_V is the surface density, and M_V and K_V are the densities of the integral of mean curvature and the integral of total curvature, respectively. Let W be a compact convex set of nonempty interior. Then the densities mentioned above can formally be introduced as the limits $V_V = \lim_{r\to\infty} \mathbb{E}V(\alpha \cap rW)/V(rW)$, $S_V = \lim_{r\to\infty} \mathbb{E}S(\alpha \cap rW)/V(rW)$, $M_V = \lim_{r\to\infty} \mathbb{E}M(\alpha \cap rW)/V(rW)$ and $K_V = \lim_{r\to\infty} \mathbb{E}K(\alpha \cap rW)/V(rW)$, see Mecke *et al.* (1990; p. 59f).

Clearly, the volume fraction of the component α and the pore space α^c complement one another, $V_V(\alpha) + V_V(\alpha^c) = 1$. Furthermore, under weak assumptions for α (in particular when α is almost surely morphologically open and closed with respect to all segments of S) we have $S_V(\alpha) = S_V(\alpha^c)$, $M_V(\alpha) = -M_V(\alpha^c)$, and $K_V(\alpha) = K_V(\alpha^c)$. (These relationships basically follow from the fact that the Euler number of a closed hollow sphere in d-dimensional space is equal to $1 - (-1)^d$, $d \geq 1$. For a random set α with polygonal surface the validity of the equations can be shown by means of the inclusion-exclusion formula, see Appendix.) In other words, it is sufficient to determine the quermassdensities of only one component of the microstructure. This is of practical importance because usually for binary microstructures (especially for the sandstones considered in this paper) the roles of α and α^c are exchangeable in some sense.

Spatial images of microstructures can be produced by computer assisted tomography (CT scans) and similar techniques using for example X-ray scattering, magnetic resonance, or isotope emission, see Russ (1992), Chapter 7, and Pan *et al.* (1998). Another technique of formation of

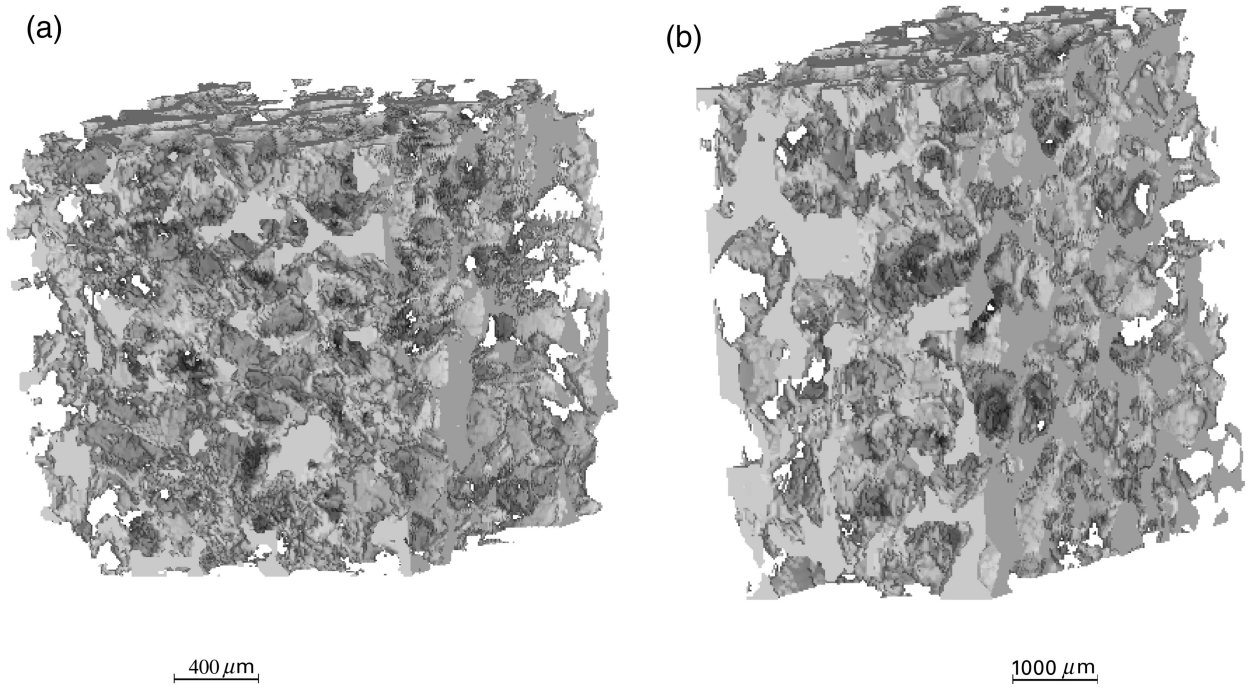

Fig. 1. Visualizations of three-dimensional images of natural sandstones (a) Berea sandstone (b) a weakly consolidated sandstone. The rock matrix is shown transparent, whereas the pore space is opaque. The three-dimensional data were obtained by computerized microtomography. The lateral resolution was uniform over all directions; $\Delta = 10$ μm for (a) and $\Delta = 30$ μm for (b). The determination of the geometric characteristics of these porous media is a prerequisite for studying transport properties such as fluid flow or sound propagation in oil reservoirs, aquifers or other materials, see Biswal *et al.* (1998).

3-dimensional images is by means of an interference confocal scanning microscope under ultrashort pulsed beam illumination, see Gu (1998). Examples of 3-dimensional images obtained by X-ray tomography are shown in Fig. 1.

One can choose between various types of discretization of 3-dimensional structures depending on the choice of the spatial lattice where we observe the structure. Examples are the cuboidal lattice, the face centred cubic lattice, and the body centred cubic lattice. Further ideas for spatial lattices that might be useful in image analysis could be taken from crystallography. However, depending on the preferred scanning technique, it is common to use cuboidal lattices, where the unit cell forms a cuboid of edge-lengths Δ_1, Δ_2 and Δ_3. The edge lengths of the unit cell are the lattice distances in the x-, y- and z-directions, respectively, and their inverses $1/\Delta_1$, $1/\Delta_2$ and $1/\Delta_3$ are said to be the lateral resolutions. The lattice distances may be small with respect to the elongation of the objects or features occurring in the α-phase.

Let a spatial lattice L be given by a sequence $\{x_{ijk}, i = 0, ..., n_1, j = 0, ..., n_2, k = 0, ..., n_3\}$ of points $x_{ijk} = (i\Delta_1, j\Delta_2, k\Delta_3)$. The spatial window W forms the cuboid $[0, n_1\Delta_1] \times [0,n_2\Delta_2] \times [0,n_3\Delta_3]$ consisting of $n := n_1n_2n_3$ cuboidal cells of volume $V_\Delta = \Delta_1\Delta_2\Delta_3$. As components of the spatial lattice we will consider vertices, edges, and faces of the cells, and the cells of the lattice itself. The (half-open) cell $[0, \Delta_1) \times [0, \Delta_2) \times [0, \Delta_3)$ is said to be the unit cell of the lattice. (For the cuboidal lattice the set S consists of 13 segments: 3 edges, 6 faces' diagonals, and the 4 spatial diagonals of the cuboid.)

The binary image $\alpha \cap L$ can be understood as a matrix $B = (b_{ijk})$ of the components $b_{ijk} = 1_\alpha(x_{ijk})$ where $1_\alpha(x)$ is the characteristic function of α. (A component b_{ijk} of a spatial image is a voxel.) Surroundings of voxels form image components of higher order, and as the most simple surrounding we consider the $2 \times 2 \times 2$-neighbourhood configurations. The $2 \times 2 \times 2$-neighbourhood configuration of the voxel b_{ijk} corresponds to the cell assigned to the lattice point x_{ijk}. It consists of the eight voxels b_{ijk}, b_{i+jk}, $b_{i,j+1,k}$, $b_{i+1,j+1,k}$, $b_{ij,k+1}$, $b_{i+1,j,k+1}$, $b_{i,j+1,k+1}$, and $b_{i+1,j+1,k+1}$.

3.1. Labelling of neighbourhood configurations

The neighbourhood configuration in a binary image can be detected by linear filtering, which can be understood as the convolution of the binary image B with a given filter mask F, the result is the grey-tone image $G = B * F$. Because we are interested in the $2 \times 2 \times 2$-neighbourhood configurations, we take a filter mask F_1, consisting of eight coefficients f_{ijk}, and if the coefficients are chosen as powers

of 2, the components g_{ijk} of the grey-tone image G are given by $g_{ijk} = \sum_{i,j,k=0}^{1} 2^{i+2j+4k} b_{ijk}$ for $i = 0, ..., n_1 - 1$, $j = 0, ..., n_2 - 1$, and $k = 0, ..., n_3 - 1$. The integer g_{ijk} can be understood as the coding of the $2 \times 2 \times 2$-neighbourhood configuration of the voxel b_{ijk}. Note that the mapping $B \rightarrow B * F_1$, is a one-to-one mapping.

Because of the size of the filter mask F_1, the grey-tone image G has 8 bits per voxel. The linear filtering is restricted to the reduced window $W_1 = [0, (n_1 - 1)\Delta_1] \times [0, (n_2 - 1)\Delta_2] \times [0, (n_3 - 1)\Delta_3]$.

We remark that the coding of neighbourhood configurations in binary images described above is not original. Its use in image processing was first suggested by the Centre de Morphologie Mathématique of the École Nationale Supérieure des Mines de Paris, see Serra (1969).

3.2. The absolute frequencies of configurations

The absolute frequencies of $2 \times 2 \times 2$-neighbourhood configuration h_k in the binary image B can be obtained by simply counting the voxels in G which have the grey-tone value g. Let δ be Kronecker's delta, i.e. $\delta_\ell(g) = 1$ for $g = \ell$, and $\delta_\ell(g) = 0$ otherwise. Then

$$h_\ell = \sum_{i=0}^{n_1-1} \sum_{j=0}^{n_2-1} \sum_{j=0}^{n_3-1} \delta_\ell(g_{ijk}), \quad \ell = 0, ..., 25$$

Clearly, the vector h can be obtained directly from the binary image B where an explicit computation and saving of the filtered image G is avoided (see Ohser & Mücklich, 2000). For example, the component h_{255} can be expressed as the number of those cells for which all vertices are in α. This can be written as

$$h_{255} = \#\left(\right.$$ 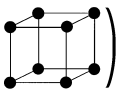 $$\left. \right)$$

where #() denotes the cardinal number of configurations in the binary image and the full disc ● indicates that a cell's vertex hits the α-phase. The estimation of h represents the 'integration step' in the algorithm, and it is easy to see that the number of operations of a proper algorithm for the computation of h is of order $O(n)$, i.e. linear in the image size.

Notice that the vector h^c of the frequencies of neighbourhood configurations of the complementary set α^c can be obtained directly from h. One gets $h^c_\ell = h_{255-\ell}$, $\ell = 0, ..., 255$.

4. Estimation of the quermassdensities

The vector $h = (h_\ell)$ comprises the data for a basic statistical analysis of the microstructure; h can be understood as the 'integrated local knowledge' about the binary image B. For example, the total sum of the h_ℓ is simply the cell number n of the lattice, $m = \sum h_\ell$ and thus the volume of the reduced window is simply obtained from $V(W_1) = V_\Delta \sum_{\ell=0}^{255} h_\ell$.

Furthermore, from the condensed information about the binary image represented by the vector h, one can estimate the geometric characteristics V_V, S_V, M_V and K_V as described below. Because the filtering is restricted to the reduced window W_1, estimates of these geometric characteristics will be 'free of edge effects'. More precisely, bias in estimates of S_V, M_V and K_V is not due to the intersection of α with the edge of the window W.

4.1. Volume and volume density

The volume of α restricted to the window W, can be estimated using the Crofton formula

$$\hat{V}(\alpha \cap W_1) = V_\Delta \sum_{i=0}^{n_1-1} \sum_{j=0}^{n_2-1} \sum_{j=0}^{n_3-1} 1_\alpha(x_{ijk})$$

where $1_\alpha(x) = \chi(\alpha \cap \{x\})$ is the characteristic function of α. This can be expressed as the sum of the volumes of those cells for which the (000)-vertices of the lattice cells hit α and the other ones are arbitrary (covered by α or its complement α^c). The codes of these configurations are odd, and hence, the sum of the h_ℓ is taken over odd index ℓ,

$$\hat{V}(\alpha \cap W_1) = V_\Delta \cdot \#\left(\right.$$ 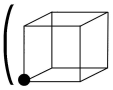 $$\left. \right) = V_\Delta \sum_{\ell=0}^{127} h_{2\ell+1}$$

where $1_a(x) = \chi(\alpha \cap \{x\})$ is the characteristic function of α. Here, the full disc ● indicates that the (000)-vertex hits α, whereas a vacant vertex means that this vertex is covered either by α or by its complement α^c.

It is immediately clear that $\hat{V}(\alpha \cap W_1)$ converges to the true value $V(\alpha \cap W_1)$ as the volume of the unit cell converges to 0, $V_\Delta \rightarrow 0$ (and $n \rightarrow \infty$). Furthermore, because α is assumed to be homogeneous (i.e. the distribution of α is invariant with respect to Euclidean motion), the estimator $V_V = 1/n \sum_{\ell=0}^{127} h_{2\ell+1}$ is unbiased for the volume density V_V of α.

By means of the usual binary bitwise Boolean operators this estimator can be rewritten as

$$V_V = \frac{1}{n} \sum_{\ell=0}^{255} h_\ell \delta_\ell(\ell \vee 1) = \frac{1}{n} \sum_{\ell=0}^{255} h_\ell [1 - \delta_\ell(\ell \wedge \neg 1]$$

$$= \frac{1}{n} \sum_{\ell=0}^{255} h_\ell [1 - \delta_0(\ell \wedge 1)]$$

It is easy to see that V_V can be expressed as an inner product of h and a vector v, $V_v = \langle h, v \rangle$, with $v_\ell = 1/n$ for components of v with odd index ℓ and $v_\ell = 0$ otherwise.

4.2. The surface density

The estimation of the surface density is based on the Crofton formula for 1-dimensional sections. For the purpose of application, now the segments in S are interpreted as 'test segments'. We introduce polar coordinates (r_v, w_v): r_v and $w_v = (\vartheta_v, \varphi_v)$ are the length and direction of the vth segment, respectively, and $\Delta_{ij} := \sqrt{(\Delta_i)^2 + (\Delta_j)^2}$ and $\Delta_{123} := \sqrt{(\Delta_1)^2 + (\Delta_2)^2 + (\Delta_3)^2}$ are the lengths of the diagonals of the ij-face and the lengths of the spatial diagonals, respectively.

For example, the segment $v = 9$ formed by the diagonal between the (000)-vertex and the (111)-vertex is of length $r_9 = \Delta_{123}$, and hence, in our lattice the total length of segments corresponding to the direction $\omega_9 = (\vartheta_9, \varphi_9)$ is equal to $n\Delta_{123}$. Consider now the area of the total projection $\wp^9$ of $\alpha \cap W$ with respect to the direction ω_9. An estimator of $\wp^9(\alpha \cap W)$ is obtained from cells which hit the boundary of α. Consider those cells for which the (000)-vertex hits α, whereas the (111)-vertex hit the complementary set α^c. We get

$$\hat{\wp}^9(\alpha \cap W) = \frac{V_\Delta}{\Delta_{123}} \# \left(\right.$$

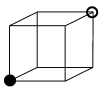

$$\left. \right).$$

Note that the ratio V_Δ/Δ_{123} is the area of the unit cell of the planar point lattice obtained by the intersection of the segments of direction ω_9 and a section plane perpendicular to these segments. The density of $\wp^9$ – the area of the total projection per unit volume $\wp_V(\omega_9)$ – can be estimated using $\wp_V(\omega_9) = \wp^9(\alpha \cap W)/V(W)$. Applied to the Euler number χ^1, Hadwiger's recursive formula yields

$$\wp_V(\omega_9) = \frac{1}{n\Delta_{123}} \sum_{\ell=0}^{255} h_\ell \delta_\ell(\ell \vee 1)[1 - \delta_\ell(\ell \vee 128)]$$

$$= \frac{1}{n\Delta_{123}} \sum_{\ell=0}^{255} h_\ell \delta_\ell(\ell \vee 1)\delta_0(\ell \vee 128)$$

As the estimator of the volume density, $\wp_V(\omega_9)$ can be rewritten as an inner product, i.e. $\wp_V(\omega_9) = \langle h, p^9 \rangle$ with a vector p^9 of components $p^9_\ell = 1/(n\Delta_{123})$ for $\ell = 1, 3, ..., 127$, and $p^9_\ell = 0$ otherwise.

For an arbitrary lattice direction ω_v, the estimator of $\wp_V(\omega_v)$ is of the form

$$\wp_V(\omega_v) = \frac{1}{nr_v} \sum_{\ell=0}^{255} h_\ell \delta_\ell(\ell \vee \kappa_{0,v})\delta_0(\ell \wedge \kappa_{1,v}), \quad v = 0, ..., 25, \tag{3}$$

where $\kappa_{0,v}$ and $\kappa_{1,v}$ are coefficients of the filter mask F_1. A survey of the quantities used in this estimator is given in Table 2. Clearly, for correspondingly chosen vectors p^v of length 256, the estimators $\wp_V(\omega_v)$ can be rewritten as $\wp_v(\omega_v) = \langle h, p^v \rangle$, $v = 0, ..., 25$.

The estimator (3) is unbiased if α is (almost surely) morphologically open as well as closed with respect to a segment of length r_v *and* direction w_v. This follows from Eq. (2) for $d = 1$. Otherwise, if α is almost surely a locally finite union of compact convex sets of nonempty interiors the asymptotic behaviour of the product $r_v \mathbb{E}\hat{\wp}_V(\omega_v)$ (considered as a function of r_v) is the same as that of the covariance function of α and, hence. the estimator $\hat{\wp}_V(\omega_v)$ is asymptotically unbiased for $\wp_V(\omega_v)$ as $r_v \to 0$.

Table 2. The directions $\omega_v = (\vartheta_v, \varphi_v)$, the lengths r_v and the coefficients $\kappa_{0,v}, \kappa_{1,v}$ of the filter mask F_1. The directions ω_v are points on the positive half-sphere. Estimates of $\wp_V(\omega_v)$ for the directions ϑ_v, φ_v with $\vartheta = \pi - \vartheta_{v-13}$, $\varphi_v = \varphi_{v-13} - \pi$, $v = 13, ..., 25$, on the negative half-sphere are obtained from (3) when exchanging $\kappa_{0,v}$ and $\kappa_{1,v}$ but leaving the distances unchanged, $r_v = r_{v-13}$, $v = 13, ..., 2$.

Test segments	v	ϑ_v	φ_v	r_v	$\kappa_{0,v}$	$\kappa_{1,v}$
Cube edges	0	$\pi/2$	0	Δ_1	1	2
	1	$\pi/2$	$\pi/2$	Δ_2	1	4
	2	0	0	Δ_3	1	16
Diagonals of faces	3	$\pi/2$	arctan Δ_2/Δ_1	Δ_{12}	1	8
	4	$\pi/2$	π – arctan Δ_2/Δ_1	Δ_{12}	2	4
	5	arccot Δ_3/Δ_1	0	Δ_{13}	1	32
	6	arccot Δ_3/Δ_1	π	Δ_{13}	2	16
	7	arccot Δ_3/Δ_2	$\pi/2$	Δ_{23}	1	64
	8	arccot Δ_3/Δ_2	$3\pi/2$	Δ_{23}	4	16
Spatial diagonals	9	arccot Δ_3/Δ_{12}	arctan Δ_2/Δ_1	Δ_{123}	1	128
	10	arccot Δ_3/Δ_{12}	π – arctan Δ_2/Δ_1	Δ_{123}	2	64
	11	arccot Δ_3/Δ_{12}	2π – arctan Δ_2/Δ_1	Δ_{132}	4	32
	12	arccot Δ_3/Δ_{12}	π + arctan Δ_2/Δ_1	Δ_{123}	8	16

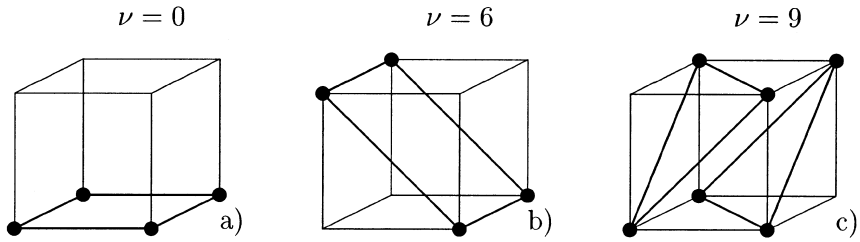

Fig. 2. Examples of planar section profiles of the unit cell: (a) the rectangle parallel to the *xy*-plane, (b) a rectangular section profile of the unit cell, (c) two triangular section profiles of the unit cell having the same normal direction. The vertices and edges of these triangular section profiles of all lattice cells form planar graphs of the type 'hexagonal-1', Serra (1982), p. 174.

From the estimators $\wp_V(\omega_v)$, $v = 0, ..., 25$, one obtains an estimator of the surface density S_V

$$S_V = 4\sum_{v=0}^{25} c_v \wp_v(\omega_v) = 4\sum_{v=0}^{25} c_v \langle h, p^v \rangle = \langle h, s \rangle \qquad (4)$$

with $s = 4\sum_{v=0}^{25} c_v p^v$. For a C routine that computes S_V from h, see Ohser & Mücklich (2000).

Equation (4) is a discrete version of Crofton's formula $S(X) = 4\int \wp^{\omega}(X)\mu(d\omega)$, see Table 1. The coefficients c_v are positive weights satisfying $\sum c_v = 1$, and the accuracy of estimation is a question of the choice of the weights c_v, which depend on the underlying quadrature rule used in the numerical computation of the rotatory integral in the Crofton formula.

Given a direction ω_v, the weight c_v depends on the distances between ω_v and its neighbouring directions. One can determine the weights as follows: Divide the unit sphere Ω into the Voronoi cells with respect to the set of directions $\{\omega_v,\ v = 0, ..., 25\}$. Then the obvious choice for c_v is the relative area of the corresponding Voronoi cell, $4\pi c_v =$ 'the area of the vth Voronoi cell'. Clearly, $c_{v+13} = c_v$. In particular, if the unit cell is a cube (i.e. $\Delta_1 = \Delta_2 = \Delta_3$) then $c_v = 0.045\,778$ for $v = 0,\ 1,\ 2$, $c_v = 0.036\,981$ for $v = 3, ... , 8$, and $c_v = 0.035\,196$ for $v = 9, ... , 12$. Because the fineness of discretization of the directions does not depend on the lattice distances, the estimator (4) is normally biased for anisotropic α even as $\Delta_{123} \to 0$. However, if isotropy of α can be assumed then it is asymptotically unbiased as $\Delta_{123} \to 0$, cf. also the discussion in Serra (1982), p. 220f, and Sandau & Hahn (1993).

4.3. The specific integral of mean curvature

From the Crofton formula for the integral of mean curvature, it immediately follows that the determination of the integral of mean curvature in three-dimensional space reduces to measurement in two-dimensional section planes through the specimen. In the cuboidal lattice, there are 13 planes associated with different normal directions and hitting three or four vertices of the cells. The corresponding planar section profiles of the unit cell form rectangles or triangles. Examples are shown in Fig. 2, and a survey of all section profiles is given in Table 3.

In the section planes corresponding to the normal directions ω_v, $v = 0, ..., 8$, the vertices and edges of the section profiles form a (planar) graph of rectangular cells; for $v = 9, ..., 12$ the vertices and edges of the section profiles form a triangular graph.

Let $\chi^2(\omega_v)$ denote the Euler number corresponding to the normal direction ω_v of a section plane that hits three or four vertices of a cell. As a consequence of a twofold application of Hadwiger's formula, the planar Euler number $\chi^2(\omega_v)$ can be estimated by a simple counting of neighbourhood configurations. For example, for $v = 6$, Euler's relation implies that

$$\hat{\chi}^2(\omega_6) = \#\left(\right) - \#\left(\right) - \#\left(\right) + \#\left(\right),$$

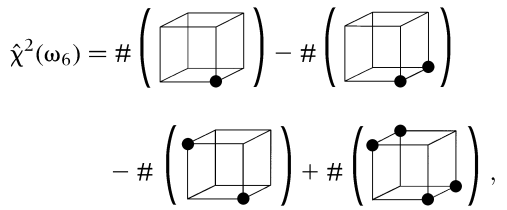

Ohser *et al.* (1998). One can easily verify that this formula reduces to

$$\hat{\chi}^2(\omega_6) = \#\left(\right) - \#\left(\right) + \#\left(\right).$$

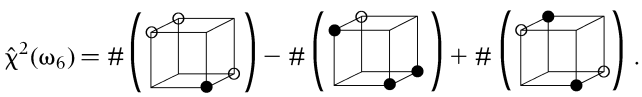

Further simplification arises if we add the spatial diagonal between the (100)-vertex and the (011)-vertex (a diagonal of the section rectangle). Then the rectangular unit cell of the planar graph under consideration is tessellated into two triangles and the last term of the previous equation vanishes, so the Euler number for the modified planar graph can be estimated using

$$\hat{\chi}^2(\omega_6) = \#\left(\right) - \#\left(\right).$$

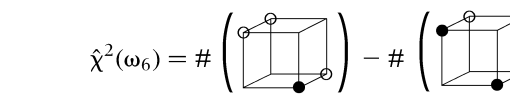

This triangulation preserves the relationship $M_V(\alpha) = -M_V(\alpha^c)$.

Let a_6 denote the area of the rectangular cell. then the density estimator of the Euler number is $\chi_A(\omega_6) = \chi^2(\omega_6)/n a_6$

Table 3. The directions $\omega_v = (\vartheta_v, \varphi_v)$, the areas a_v, and coefficients $\kappa_{0,v}$, $\kappa_{1,v}$, $\kappa_{2,v}$, $\kappa_{3,v}$ of the filter mask F_1. Notice that for $v = 13, ..., 21$ the constants can be obtained from $\vartheta_v = \pi - \vartheta_{v-13}$, $\varphi_v = \varphi_{v-13} - \pi$, $\kappa_{0,v} = \kappa_{3,v-13}$, $\kappa_{1,v} = \kappa_{2,v-13}$, $\kappa_{2,v} = \kappa_{1,v-13}$, $\kappa_{3,v} = \kappa_{0,v-13}$ and $a_v = a_{v-13}$.

Test areas	v	ϑ_v	φ_v	a_v	$\kappa_{0,v}$	$\kappa_{1,v}$	$\kappa_{2,v}$	$\kappa_{3,v}$
Faces	0	0	0	$\Delta_1\Delta_2$	1	2	4	8
of the cuboid	1	$\pi/2$	$\pi/2$	$\Delta_1\Delta_3$	1	2	16	32
	2	$\pi/2$	0	$\Delta_2\Delta_3$	1	4	16	64
Diagonal	3	arctan Δ_3/Δ_2	$3\pi/2$	$\Delta_3\Delta_{12}$	1	2	64	128
rectangles	4	arctan Δ_3/Δ_2	$\pi/2$	$\Delta_3\Delta_{13}$	4	16	8	32
	5	arctan Δ_3/Δ_1	π	$\Delta_2\Delta_{13}$	1	32	4	128
	6	arctan Δ_3/Δ_1	0	$\Delta_2\Delta_{13}$	2	8	16	64
	7	$\pi/2$	θ_{12}	$\Delta_1\Delta_{23}$	2	4	32	64
	8	$\pi/2$	$\pi - \theta_{12}$	$\Delta_1\Delta_{23}$	1	16	8	128
Diagonal	9	θ_{123}	$\pi + \theta_{12}$	$2A_{123}$	1	64	32	–
triangles	10	θ_{123}	$2\pi - \theta_{12}$	$2A_{123}$	2	16	128	–
	11	θ_{123}	θ_{12}	$2A_{123}$	8	64	32	–
	12	θ_{123}	$\pi - \theta_{12}$	$2A_{123}$	4	16	128	–
	22	$\pi - \theta_{123}$	θ_{12}	$2A_{123}$	2	4	128	–
	23	$\pi - \theta_{123}$	$\pi - \theta_{12}$	$2A_{123}$	8	1	64	–
	24	$\pi - \theta_{123}$	$\pi + \theta_{12}$	$2A_{123}$	2	4	16	–
	25	$\pi - \theta_{123}$	$2\pi - \theta_{12}$	$2A_{123}$	8	1	32	–

and thus

$$\chi_A(\omega_6) = \frac{1}{na_6}\left[\sum_{\ell=0}^{255} h_\ell \delta_\ell(\ell \vee 2)\delta_0(\ell \wedge 8)\delta_0(\ell \wedge 16)\delta_0(\ell \wedge 64) - \sum_{\ell=0}^{255} h_\ell \delta_\ell(\ell \vee 2)\delta_\ell(\ell \vee 8)\delta_\ell(\ell \vee 16)\delta_0(\ell \wedge 64)\right]$$

In the general case we obtain for the rectangular section profiles of the unit cell

$$\chi_A(\omega_v) = \frac{1}{na_v} \times \left[\sum_{\ell=0}^{255} h_\ell \delta_\ell(\ell \vee \kappa_{0,v})\delta_0(\ell \wedge \kappa_{1,v})\delta_0(\ell \wedge \kappa_{2,v})\delta_0(\ell \wedge \kappa_{3,v}) - \sum_{\ell=0}^{255} h_\ell \delta_\ell(\ell \vee \kappa_{0,v})\delta_\ell(\ell \vee \kappa_{1,v})\delta_\ell(\ell \vee \kappa_{2,v})\delta_0(\ell \wedge \kappa_{3,v})\right]$$

$v = 0, ..., 8$, where $\kappa_{0,v}$, $\kappa_{1,v}$, $\kappa_{2,v}$ and $\kappa_{3,v}$ are the coefficients of the filter mask F_1, relating to the vertices of the rectangular section profiles. For the triangular section profiles

$$\chi_A(\omega_v) = \frac{1}{na_v}\left[\sum_{\ell=0}^{255} h_\ell \delta_\ell(\ell \vee \kappa_{0,v})\delta_0(\ell \wedge \kappa_{1,v})\delta_0(\ell \wedge \kappa_{2,v}) - \sum_{\ell=0}^{255} h_\ell \delta_\ell(\ell \vee \kappa_{0,v+13})\delta_\ell(\ell \vee \kappa_{1,v+13})\delta_\ell(\ell \vee \kappa_{2,v+13})\right],$$

$v = 9, ..., 12$, cf. Serra (1982), p. 233. The constants used in these formulae are given in Table 3, where A_{123} denotes the area of the triangles, $A_{123} = \sqrt{s(s-\Delta_{12})(s-\Delta_{13})(s-\Delta_{23})}$ with $s = \Delta_{12} + \Delta_{13} + \Delta_{23})/2$ (Heron formula). The constants θ_{12} and θ_{123} are the azimuth angle and the zenith angle of the normal direction of the section triangles, respectively, $\theta_{12} = \arctan(\Delta_2/\Delta_1)$ and $\theta_{123} = \arctan[\Delta_3/(\Delta_1\cos\theta_{12})]$. The coefficients $\kappa_{0,v}$, $\kappa_{1,v}$, $\kappa_{2,v}$ and $\kappa_{3,v}$ are associated with the vertices of the section polygons and the directions ω_v, are points on the positive half-sphere.

We firstly refer to the meaning of the estimates $\chi_A(\omega_v)$ in the characterization of structural anisotropy. Furthermore, as a discrete version of Crofton's formula for M_V in Table 1 one obtains from the estimators $\chi_A(\omega_v)$ an estimator of the specific integral of mean curvature,

$$M_V = 2\pi\sum_{v=0}^{255} c_v \chi_A(\omega_v)$$

where the c_v are suitable positive weights satisfying $\sum c_v = 1$, cf. also the discussion in the previous section, and v indexes the discrete directions ω_v. For uniform lattice spacing the weights are $c_v = 0.0457785$, $v = 0, 1, 2$, $c_v = 0.036981$, $v = 3,..., 8$, and $c_v = 0.035196$, $v = 9, ..., 13$.

From Eqs (5) and (6) it follows that M_V can be rewritten as $M_V = \langle h, t\rangle$ where the vector t depends on the lateral resolution and the quadrature rule applied in the computation of the outer integral in the corresponding Crofton formula. Thus, the algorithm of computing M_V from B is also of order $O(n)$. For a C-routine see Ohser & Mücklich (2000).

Table 4. The vector v used in the estimator K_V. The coefficients listed are proportional to that of v; the multiplicative constant is $6nV_\Delta/\pi$.

0	3	3	0	3	0	0	−3	3	0	0	−3	0	−3	−3	0	0	15
3	0	0	−3	0	−3	−3	−6	−6	−9	−9	−6	−9	−10	−8	−3	16	31
3	0	0	−3	− 6	−9	−9	−10	0	−3	−3	−6	−9	−8	−6	−3	32	47
0	−3	−3	0	− 9	−6	−8	−3	−9	−8	−10	−3	−16	−9	−9	0	48	63
3	0	−6	−9	0	−3	−9	−6	0	−3	−9	−8	−3	−6	−10	−3	64	79
0	−3	−9	−10	− 3	0	−8	−3	−9	−8	−16	−9	−6	−3	−9	0	80	95
0	−3	−9	−8	− 9	−8	−16	−9	−3	0	−8	−3	−8	−3	−9	0	96	111
−3	−6	−6	−3	− 10	−3	−9	0	−8	−3	−9	0	−9	0	−6	3	112	127
3	−6	0	−9	0	−9	−3	−8	0	−9	−3	−10	−3	−6	−6	−3	128	143
0	−9	−3	−8	− 3	−8	0	−3	−9	−16	−8	−9	−8	−9	−3	0	144	159
0	−9	−3	−6	− 9	−16	−8	−9	−3	−8	0	−3	−10	−9	−3	0	160	175
−3	−10	−6	−3	− 8	−9	−3	0	−6	−9	−3	0	−9	−6	0	3	176	191
0	−9	−9	−16	− 3	−10	−8	−9	−3	−8	−6	−9	0	−3	−3	0	192	207
−3	−6	−8	−9	− 6	−3	−3	0	−10	−9	−9	−6	−3	0	0	3	208	223
−3	−8	−10	−9	− 6	−9	−9	−6	−6	−3	−3	0	−3	0	0	3	224	239
0	−3	−3	0	− 3	0	0	3	−3	0	0	3	0	3	3	0	240	255

4.4. The specific integral of total curvature

Finally, we remark that an estimator K_V of the density of the integral of total curvature K_V can also be expressed as an inner product of h *and* a vector v, i.e.

$$K_V = \langle h, v \rangle$$

where the vector v is independent of the observed set $\alpha \cap W$. The computation of v is described in Nagel *et al.* (2000) and Ohser & Mücklich (2000). The coefficients of v are listed in Table 4. These coefficients have been computed by means of Hadwiger's formula and preserving that the neighbourhood relationships of the lattice points for the set a and the complementary set α^c are of the same complexity. (In the present case the vector v corresponds to the so-called '14-neighborhood' in the cuboidal lattice.)

As a consequence of the use of Eq. (2) in the computation of v, the estimator is unbiased for K_V if α is morphologically open and morphologically closed for all $s \in S$.

4.5. Example of application

As an example of application we estimate the quermassdensities of natural sandstones shown in Fig. 1. A survey of the results is given in Table 5, where α denotes the rock matrix and the complementary set α^c is the pore space.

Clearly, the differences between the estimates of the quermassdensities result from differences between both microstructures. However, it should be noted that there also the lateral resolutions are different so that the estimates are of limited comparability only.

The estimation variances of the estimates of the volume densities can be computed using the formula $\operatorname{var} V_V \approx pow(o)/V(W_1)$ where $\operatorname{pow}(t)$, $t \in \mathbb{R}^3$, is the spectral density of α and $\operatorname{pow}(o)$ is called the 'range of interaction' or 'asymptotic variance', see, e.g. Serra (1982). Assuming 'exponential covariance', one obtains for an enlarged window

$$\operatorname{var} \hat{V}_V \approx \frac{512\pi V_V^4(1 - V_V)^4}{S_V^3 V(W_1)},$$

see Ohser & Mücklich (2000, p. 146). If we replace V_V and S_V on the right-hand side by their estimates, we get $\sqrt{\operatorname{var} \hat{V}_V} \approx 0.5\%$ for the Berea sandstone and $\sqrt{\operatorname{var} \hat{V}_V} \approx 1.7\%$ for the weakly consolidated sandstone. This method of estimating the statistical error is simple but very elegant. Unfortunately, until now there exist no analogous methods for the other quermassdensities.

5. Concluding remarks

The boundary of α can be modelled as a smooth spatial surface, which separates the set of lattice points covered by α from the complementary set of lattice points. Modelling such a surface is a real problem which can be solved by

Table 5. A survey of the quermassdensities for the rock matrix of the specimens shown in Figs l(a) and (b).

	Berea	Weakly consolidated
voxels	128 × 128 × 128	128 × 128 × 73
Δ (μm)	10	30
$V(W_1)$ (mm^3)	2.048	31.4
V_V (%)	82.2	75.3
S_V (mm^{-1})	13.860	5.918
M_V (mm^{-2})	−252	−25.0
K_V (mm^{-3})	−18982	−674

techniques well known from computer graphics. Given a smooth surface, a straightforward algorithm for computing the surface area as well as the two curvature integrals could be based on conventional integration over this surface, see, e.g. Cohen-Or & Kaufmann (1995).

The technique presented in this paper is quite different from this approach. Due to Crofton's intersection formulae and Hadwiger's recursive definition of the Euler number, we are able to estimate the surface area and the two curvature integrals without having to localize the surface, and hence, we do not need any model for the smoothness of the surface. Our technique is closely related to the method of estimating the surface density from the correlation function, as first discussed by Debye *et al.* (1957). However, this technique does not evaluate the full correlation function, and it involves a filtering that is not used when calculating correlation functions. The problem reduces to the numerical integration of functions defined on the unit sphere. For both approaches the accuracy of estimation depends on the numerical accuracy of integration (i.e. it depends on the chosen quadrature rule).

The length of the vector of absolute frequencies is equal to the total number of different configurations occurring in the binary image. Hence, the vector length does not depend on the image size itself, it depends only on the size of the applied filter mask. This is a clear advantage over other techniques. in particular, for large spatial images or when data have to be accumulated from a series of images of the same specimen but of different sizes. Hence, the 'analysis step' can be performed very easily and quickly, and the algorithm for the statistical estimation of the geometric characteristics can be presented in a well-structured form. As the estimators of the quermassdensities can be expressed in terms of the vector h, algorithms that compute these estimates for a binary image B are of order $O(n)$ where n is the number of voxels.

In principle, the size of the filter mask could be increased. In particular, the mask F_1 can be replaced by the $3 \times 3 \times 3$ filter mask $F_2 = (f_{ijk})$ with $f_{ijk} = 2^{i+3j+9k}$ for $i, j, k = 0, 1, 2$. Then the corresponding unit cell consists of eight cubes and the number of directions ω_v in the unit cell is 54 but the corresponding lattice distances r_v increase too. This means that angular resolution can be improved while the lateral resolution is reduced. In other words, one can choose between high digital resolution or high directional resolution. The errors in the estimates corresponding to the lateral resolution and the directional resolution behave in an opposite way. Therefore, the optimal size of the filter mask depends on the 'regularity of the surface' of α as well as on the 'degree of anisotropy'.

Depending on the size of the corresponding filter mask, the amounts of memory space for the obtained grey-tone image as well as the grey-tone histogram can become very large. (Applying F_2, the filtered image G would be of size $n2^{19}$ byte.) Therefore, in the implementation of the algorithms for larger filter masks, the explicit representation of the filtered image G and the vector h should be avoided, cf. Ohser *et al.* (1998) where this problem has been discussed in detail for the analysis of planar images.

Protecting the unbiasedness of the estimators of the quermassdensities we often suppose that α is almost surely morphologically open and morphologically closed. Clearly, for practical application this requirement seems to be too strong. However, this more technical condition is not a necessary but a sufficient condition for the unblasedness of the estimators, cf. the discussion in Ohser & Nagel (1996) and Nagel *et al.* (2000). Nevertheless, there are a lot of open problems concerning this condition. Is it possible to formulate some weaker conditions for α such that the estimators presented in this paper are unbiased? Can one find estimators that are unbiased for more general homogeneous random sets? How can one compute the bias of the estimators? We remark that for the 2d case there are also problems that have not yet been solved in their whole complexity, see also Ohser *et al.* (1998).

Acknowledgement

The authors J.O. and R.H. are grateful to the Stiftung Rheinland-Pfalz für Innovation and Deutsche Forschungsgemeinschaft for financial support.

References

Biswal, B., Manwart, C. & Hilfer. R. (1998) Three-dimensional local porosity analysis of porous media. *Physika A*, **255**, 221–241.

Cohen-Or, D. & Kaufman, A. (1995) Fundamentals of surface voxelization. *Graph Models Image Processing*, **57**, 453–461.

Debye, R., Anderson, H.R.K. & Brumberger, H. (1957) Scattering by an inhomogeneous solid 11: The correlation function and its application. *J. Appl. Phys.* **28**, 679–683.

Gu, M. (1998) Image formation in femtosecond confocal interference microscopy. *Microsc. Microanal.* **4**, 63–71.

Hilfer, R. (1992a) Geometric and dielectric characterization of porous media. *Phys. Rev.* **1344**, 60–75.

Hilfer, R. (1992b) Local porosity theory for flow in porous media. *Phys. Rev.* **B45**, 7115–7121.

Hilfer, R. (1996) Transport and relaxation phenomena in porous media. *Adv. Chem. Phys.* **XCII**, 299–424.

Lohmann, G. (1998) *Volumetric Image Analysis.* Wiley & Sons, Chichester.

Mecke, J., Schneider, R., Stoyan D., & Weil, W. (1990) *Stochastische Geometrie.* Birkhäuser, Basel.

Nagel, W., Ohser, J. & Pischang, K. (2000) An integral-geometric approach for the Euler–Poincaré characteristic of spatial images. *J. Microsc.* **198**, 54–62.

Ohser, J., Steinbach, B. & Lang, C. (1998) Efficient texture analysis of binary images. *J. Microsc.* **192**, 20–28.

Ohser, J. & Mücklich, F. (2000) *Statistical Analysis of Microstructures in Materials Science*. J. Wiley & Sons, Chichester.

Ohser. J. & Nagel, W. (1996) The estimation of the Euler–Poincaré characteristic from observations on parallel sections. *J. Microsc.* **184**, 117–126.

Pan, S., Liou, W., Shili, A., Park, M.-S., Wang, G., Newberry, S.P., Kim, H., Shinozaki, D.M. & Cheng, P.-C. (1998) Experimental system for X-ray cone-beam microtomography. *Microsc. Microanal.* **4**, 56–62.

Russ, J.C. (1992) *The Image Processing Handbook*. CRC Press, Boca Raton, Florida.

Sandau, K. & Hahn, U. (1993) Some remarks on the accuracy of surface area estimation using the spatial grid. *J. Microsc.* **173**, 67–72.

Schneider, R. & Weil, W. (2000) *Stochastische Geometrie.* Teubner, Stuttgart.

Schneider, R. (1993) *Convex Bodies: the Brunn-Minkowski Theory. Encyclopedia of Mathematics and Its Application*, Vol. 44. Cambridge University Press, Cambridge.

Serra, J. (1969) *Introduction à la Morphologie Mathématique.* Cahiers du Centre de Morphologie Mathématique, Booklet no. 3. ENSMP, Fontainbleau.

Serra, J. (1982) *Image Analysis and Mathematical Morphology*, Vol. 1. Academic Press, London.

Widjajakususina, 1., Biswal, B. & Hilfer, R. (1999) Quantitative prediction of effective material properties of heterogeneous media. *Comp. Mat. Set.* **16**, 70–81.

Appendix

Let X be a d-dimensional simplex having the independent vertices $x_0, \ldots, x_d \in \mathbb{R}^d$. As X is compact and convex, the Euler number is $\chi(X) = 1$. The simplex X is the intersection of $d + 1$ closed halfspaces $H_0, \ldots, H_d$, $X = \cap_{i=0}^{d} H_i$. Given a compact convex set W such that the simplex X is subset of the interior W^{int} of W, $X \subset W^{\text{int}}$. Then the closures $(W\backslash H_i)^{\text{cl}}$ of the sets $W\backslash H_i$ are compact and convex, and for the set difference $W\backslash X$ we obtain

$$W\backslash X = \bigcup_{i=0}^{d} W\backslash H_i.$$

From the inclusion–exclusion formula it follows,

$$\chi((W\backslash X)^{cl}) = \sum_{i=1}^{d} (-1)^{i+1} \binom{d+1}{i},$$

i.e. $\chi((W\backslash X)^{cl}) = 0$ if d is even, and $\chi((W\backslash X)^{cl}) = 2$ if d is odd. Hence, $\chi((W/X)^{cl})$ can be rewritten as

$$\chi((W\backslash X)^{cl}) = \chi(W) + (-1)^{d+1}\chi(X). \tag{8}$$

Now let X be the union of two simplices X_1, and X_2 where the interior of the intersection is nonempty $(X_1 \cap X_2)^{\text{int}} \neq \emptyset$. Then $X_1 \cap X_2$ is a complex polyhedron and thus $\chi((W\backslash(X_1 \cap X_2))^{cl}) = \chi(W) + (-1)^{d+1}\chi(X_1 \cap X_2)$. This implies

$$\begin{aligned}
\chi((W\backslash X)^{cl}) &= \chi((W\backslash(X_1 \cup X_2))^{cl}) = \chi(((W\backslash X_1) \cap (W\backslash X_1))^{cl}) \\
&= \chi((W\backslash X_1)^{cl}) + \chi((W\backslash X_2)^{cl}) \\
&\quad - \chi(((W\backslash X_1) \cup (W\backslash X_2))^{cl}) \\
&= \chi((W\backslash X_1)^{cl}) + \chi((W\backslash X_2)^{cl}) \\
&\quad - \chi((W\backslash(X_1 \cap X_2))^{cl}) \\
&= \chi(W) + (-1)^{d+1}\chi(X_1) \\
&\quad + \chi(W) + (-1)^{d+1}\chi(X_2) \\
&\quad - \chi(W) - (-1)^{d+1}\chi(X_1 \cap X_2)
\end{aligned}$$

and hence

$$\chi((W\backslash(X_1 \cup X_1))^{cl}) = \chi(W) + (-1)^{d+1}\chi(X_1 \cup X_2).$$

Since any convex polyhedron is a union of simplices, from the last last formula it follows that Eq. (8) is valid also if X is a finite union of compact convex polyhedra. Setting $\chi(\mathbb{R}^d) = 1$ we get $\chi((X^c)^{cl}) = \chi((\mathbb{R}^d \backslash X)^{cl}) = 1 + (-1)^{d+1}\chi(X)$.

Let α be a three-dimensional random set and assume that α is homogeneous and its realizations are almost surely locally finite unions of compact convex polyhedra. Then the density $\chi_V(\alpha) := \lim_{r\to\infty} \mathbb{E}\chi(\alpha \cap rW)/V(rW)$ exist, and using the local version of the Euler characteristic, see Schneider & Weil (2000), one can show that

$$\begin{aligned}
\chi_V(\alpha^c) &:= \lim_{r\to\infty} \frac{\mathbb{E}\chi((\mathbb{R}^3\backslash\alpha)^{cl} \cap rW)}{V(rW)} \\
&= \lim_{r\to\infty} \frac{1 + \mathbb{E}\chi(\alpha \cap rW)}{V(rW)} = \chi_V(\alpha).
\end{aligned}$$

The identity $K_V(\alpha^c) = K_V(\alpha)$ follows from $K_V = 4\pi\chi_V$. Finally, for any (r,ω) the planar section $\alpha \cap E_{r,\omega}$, forms a planar random set which is almost surely a locally finite union of compact convex polygons. Then the densities

$$\chi_A(\alpha \cap E_{r,\omega}) := \lim_{s\to\infty} \frac{\mathbb{E}\chi(\alpha \cap sW \cap E_{r,\omega})}{A(sW \cap E_{r,\omega})}$$

and

$$\chi_A(\alpha^c \cap E_{r,\omega}) := \lim_{s\to\infty} \frac{\mathbb{E}\chi((E_{r,\omega}\backslash\alpha)^{cl} \cap sW)}{A(sW \cap E_{r,\omega})}$$

exist and with $d = 2$ from Eq. (8) we obtain the relationship

$$\chi_A(\alpha^c \cap E_{r,\omega}) = -\chi_A(\alpha \cap E_{r,\omega}), \quad (r,\omega) \in \mathbb{R}^3.$$

Using the Cauchy formula, the homogeneity of α implies $M_V(\alpha) = 2\pi\int_\Omega \chi_A(\alpha \cap E_{r,\omega})\mu(d\omega)$ and $M_V(\alpha^c) = 2\pi\int_\Omega \chi_A(\alpha^c \cap E_{r,\omega})\mu(d\omega)$ for $r \in e_{o,\omega}$, which yields the fundamental equation $M_V(\alpha^c) = -M_V(\alpha)$.